



Short communication

## Towards small molecule inhibitors of mono-ADP-ribosyltransferases



Torun Ekblad <sup>a,1</sup>, Anders E.G. Lindgren <sup>b,1</sup>, C. David Andersson <sup>b</sup>, Rémi Caraballo <sup>b</sup>, Ann-Gerd Thorsell <sup>a</sup>, Tobias Karlberg <sup>a</sup>, Sara Spjut <sup>b</sup>, Anna Linusson <sup>b</sup>, Herwig Schüler <sup>a,\*</sup>, Mikael Elofsson <sup>b,\*</sup>

<sup>a</sup> Department of Medicinal Biochemistry and Biophysics, Karolinska Institutet, SE-17177 Stockholm, Sweden

<sup>b</sup> Department of Chemistry, Umeå University, SE-90187 Umeå, Sweden

## ARTICLE INFO

## Article history:

Received 3 February 2015

Received in revised form

18 March 2015

Accepted 31 March 2015

Available online 1 April 2015

## Keywords:

Mono-ADP-ribosyltransferase

mART

Poly(ADP-ribose) polymerase

Diphtheria toxin-like ADP-

ribosyltransferase

ARTD inhibitor

PARP inhibitor

## ABSTRACT

Protein ADP-ribosylation is a post-translational modification involved in DNA repair, protein degradation, transcription regulation, and epigenetic events. Intracellular ADP-ribosylation is catalyzed predominantly by ADP-ribosyltransferases with diphtheria toxin homology (ARTDs). The most prominent member of the ARTD family, poly(ADP-ribose) polymerase-1 (ARTD1/PARP1) has been a target for cancer drug development for decades. Current PARP inhibitors are generally non-selective, and inhibit the mono-ADP-ribosyltransferases with low potency. Here we describe the synthesis of acylated amino benzamides and screening against the mono-ADP-ribosyltransferases ARTD7/PARP15, ARTD8/PARP14, ARTD10/PARP10, and the poly-ADP-ribosyltransferase ARTD1/PARP1. The most potent compound inhibits ARTD10 with sub-micromolar IC<sub>50</sub>.

© 2015 The Authors. Published by Elsevier Masson SAS. This is an open access article under the CC BY license (<http://creativecommons.org/licenses/by/4.0/>).

## 1. Introduction

Diphtheria toxin-like ADP-ribosyl transferases (ARTDs), better known as poly(ADP-ribose) polymerases (PARPs), use nicotinamide adenine dinucleotide (NAD<sup>+</sup>) as co-substrate to transfer ADP-ribose to their target proteins [1,2]. PARPs catalyze the formation of linear or branched poly(ADP-ribose) chains, dynamic structures that are recognized by a number of reader domains and broken down by poly(ADP-ribose) glycohydrolases [3]. A large subset of the PARP family catalyzes mono-ADP-ribosylation but not chain elongation [1,4,5] (Fig. 1A). Recently, functional information has been accumulating on these mono-ADP-ribosyltransferases (mARTDs) [6,7]. Most of them combine an ADP-ribosyltransferase domain with ADP-ribose binding macro domains or WWE-domains, CCCH-type zinc finger domains, and other protein–protein interaction modules. The macro domain containing ARTD7/PARP15, ARTD8/PARP14 and ARTD9/PARP9 are overexpressed in diffuse large B-cell

lymphoma, and ARTD8 is implicated in the regulation of gene transcription [8–10]. ARTD10 is a component in the NF-κB signaling pathway by directly modifying NEMO [11]. Specific mono-ADP-ribose reader and eraser domains are also beginning to be recognized [3,12].

Numerous drug discovery programs have been dedicated to PARP inhibitors [13,14]. The predominant therapeutic area is cancer, where inhibition of ARTD1 is beneficial, in particular in combination with DNA damage repair deficiencies [15,16]. The majority of current PARP inhibitors are nicotinamide mimics that display broad inhibition of PARPs *in vitro* [17,18]. Less attention has been put on identification of selective inhibitors of mARTDs. Recently Venkannagiri et al. screened a library consisting of 502 natural products and identified several ARTD10/PARP10 inhibitors with varying potencies [19]. The potential of these inhibitors remains to be established since the compounds were not characterized by a full dose-response analysis and profiling against other members of the ARTD/PARP enzyme family. We have previously identified structural features in both enzymes and small molecule inhibitors that might facilitate the development of selective PARP inhibitors [17]. Based on that analysis we have developed and presented virtual screening procedures to identify compounds **1** and **2** as starting points for development of potent and selective mARTD inhibitors

\* Corresponding authors.

E-mail addresses: [herwig.schuler@ki.se](mailto:herwig.schuler@ki.se) (H. Schüler), [mikael.elifsson@chem.umu.se](mailto:mikael.elifsson@chem.umu.se) (M. Elofsson).

<sup>1</sup> These authors contributed equally to this work.

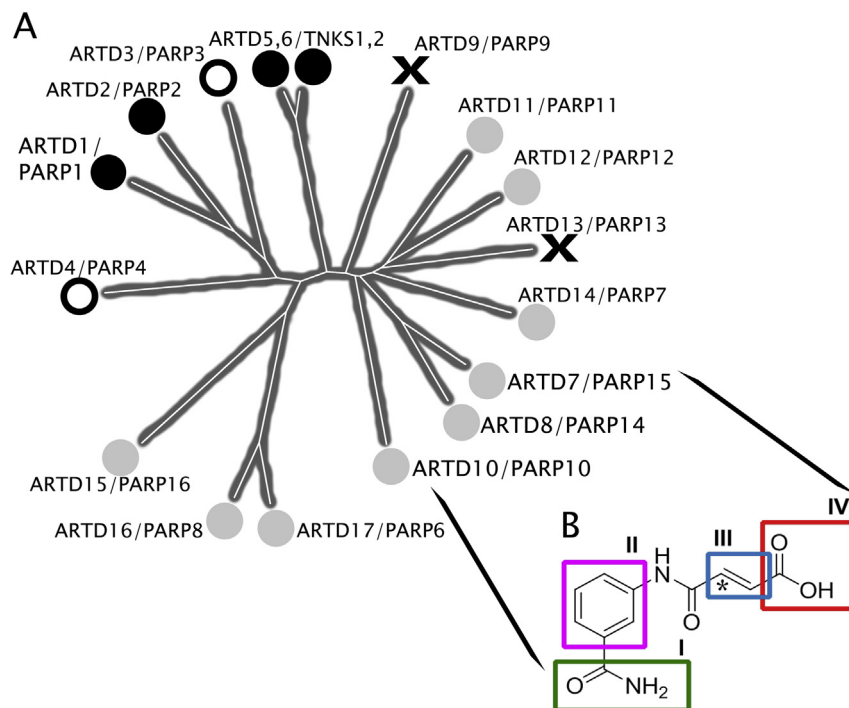


**Fig. 1.** A: Phylogenetic tree of the human PARP-family ADP-ribosyltransferases. Enzymatic activities are indicated by symbols (black circles, poly-ADP-ribosylation; grey circles, mono-ADP-ribosylation; rings, likely mono-ADP-ribosylation; crosses, putative inactive enzymes), B: Structural modifications made in the current program to target ARTD7, -8, and -10, on primary hit compound **1** (cf. Table 1): positions I (amide), II (benzene ring), III (alkene), and IV (terminal carboxylic acid).

(Table 1) [20]. Here we describe a medicinal chemistry program with the aim to develop potent inhibitors of ARTD7, -8, and -10.

## 2. Results and discussion

Compounds **1** and **2** (Table 1) were discovered in a virtual screen and verified as binders to ARTD7 and -8 by isothermal titration calorimetry and x-ray crystallography [20]. We have now developed robust enzymatic assays for these two enzymes as well as ARTD10 and could establish that both compounds indeed inhibit the enzymatic activity of all three enzymes (Table 1). We found that **1** and **2** are more potent as ARTD10 inhibitors, with  $IC_{50}$  values of 1.3  $\mu$ M and 10.6  $\mu$ M respectively. Based on these promising results a set of analogues of **1** and **2** (Table 1) was designed to explore the structure-activity relationship (SAR) for inhibition of ARTD7, -8 and -10 in relation to ARTD1. The compounds can readily be synthesized from commercially available building blocks as outlined in Scheme 1. Aminobenzamides are reacted with carboxylic anhydrides or carboxylic acids to give target compounds, and for a subset the resulting carboxylic acid is further functionalized to esters or amides. Fig. 1B illustrates the moieties explored within the SAR series and Table 1 presents enzymatic inhibition data against ARTD7, -8 and -10 as well as ARTD1.

Previous data and crystal structures (e.g. Ref. [17]) indicated that the benzamide in position I was likely to be crucial for enzyme inhibition, and many known PARP inhibitors contains a benzamide functionality that mimics the nicotinamide in  $NAD^+$  [21]. The amide forms a bifurcated hydrogen bond interaction to a conserved backbone glycine in the active site of the enzymes. Comparison of existing crystal structures indicated that the volume that harbors the amide is similar between ARTD1 and the mARTDs, but there are significant local differences in amino acid composition. To address selectivity between ARTD1 and the mARTDs, we decided to

investigate whether the amide position I (Fig. 1B) is equally important for inhibition of ARTD7, -8 and -10. Moving the amide to position 4 relative to the anilide (**3**) abolished inhibition, which indicates that the amide in this position is crucial for inhibition of both mono- and poly-ADP-ribosylation (Table 1). Functionalization of the amide itself influenced the solubility dramatically, and compounds **4–6** could not be analyzed in the enzymatic assay. Subsequently, additional substituents were introduced on benzene ring II (Fig. 1B, **7**, **8**, and **9**) and also these modifications abolished inhibition, indicating that the binding site accommodating the benzene ring is restricted in size.

The role of the double bond in position III (Fig. 1B) was explored by various modifications including saturation (**10**), addition of methyl or methoxy groups (**11**, **12**, **13** and **14**), and ring formations (**15**, **16**, and **17**). The chiral compounds **13**, **15**, and **26** were prepared and evaluated as racemates. Most of these compounds retained activity with profiles similar to those for **1** and **2**, with  $\mu$ M potency against ARTD10, ARTD7, and ARTD1. However, ARTD8 appears to be more resistant to inhibition. Saturation was well tolerated (**10**) and some alterations, such as the specific methylation in **12**, seem favorable for ARTD7 inhibition. Certain ring formations with retained cis configuration (**15**, **16**, and **17**) were relatively well tolerated. The carbon chain in position III (Fig. 1B) was then extended (**18**) and, compared to the shorter chain in **10**, this slightly decreased the inhibition of ARTD7 and -10. The importance of the carboxylic acid (position IV, Fig. 1B) was explored by modifying it into alkylated amides (**19**, **20**, **21** and **22**), a methyl ester (e.g., **23**) or ketones (**24**, **25** and **26**). To our surprise the methyl amide, **19**, with cis configuration could not be isolated using the standard synthetic procedure. Instead we attempted a solid-phase synthesis strategy according to the 9-fluorenylmethoxycarbonyl (Fmoc) protocol [22] as outlined in Scheme 2. Using this method, **19** was successfully synthesized. While this synthesis consists of more steps its overall

**Table 1**  
mARTD inhibitor structures and their inhibition of the catalytic activity of the full length enzymes ARTD1 and ARTD10, and the catalytic domains of ARTD7 and ARTD8, expressed in IC<sub>50</sub> and pIC<sub>50</sub>.

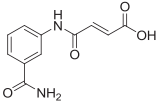
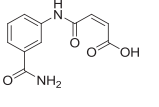
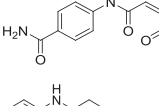
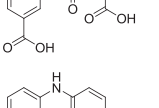
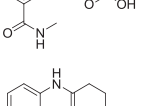
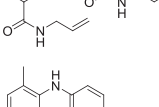
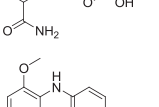
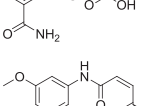
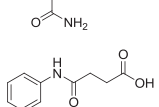
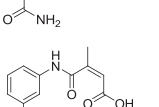
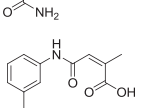
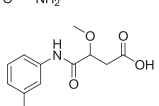
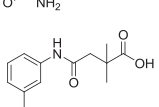
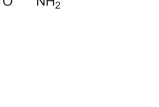
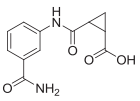
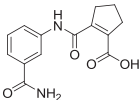
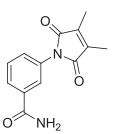
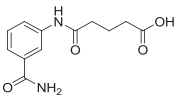
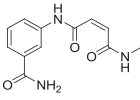
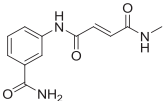
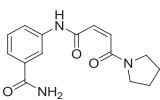
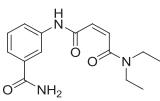
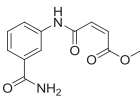
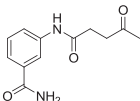
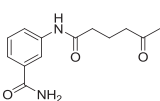
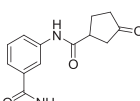
ID	Compound	ARTD10/PARP10 IC <sub>50</sub> (μM) (pIC <sub>50</sub> ± SEM <sup>a</sup> )	ARTD8/PARP14 IC <sub>50</sub> (μM) (pIC <sub>50</sub> ± SEM <sup>a</sup> )	ARTD7/PARP15 IC <sub>50</sub> (μM) (pIC <sub>50</sub> ± SEM <sup>a</sup> )	ARTD1/PARP1 IC <sub>50</sub> (μM) (pIC <sub>50</sub> ± SEM <sup>a</sup> )
1		1.3 (5.86 ± 0.10)	>20	17.8 (4.75 ± 0.06)	3.6 (5.44 ± 0.18)
2		10.6 (4.97 ± 0.12)	>20	15.8 (4.80 ± 0.09)	4.4 (5.35 ± 0.09)
3		n.i. <sup>b</sup>	n.i. <sup>b</sup>	n.i. <sup>b</sup>	>20
4		n/a <sup>c</sup>	n/a <sup>c</sup>	n/a <sup>c</sup>	n/a <sup>c</sup>
5		n/a <sup>c</sup>	n/a <sup>c</sup>	n/a <sup>c</sup>	n/a <sup>c</sup>
6		n/a <sup>c</sup>	n/a <sup>c</sup>	n/a <sup>c</sup>	n/a <sup>c</sup>
7		n.i. <sup>b</sup>	n.i. <sup>b</sup>	n.i. <sup>b</sup>	>20
8		>20	n.i. <sup>b</sup>	n.i. <sup>b</sup>	>20
9		n.i. <sup>b</sup>	n.i. <sup>b</sup>	n.i. <sup>b</sup>	>20
10		1.9 (5.72 ± 0.10)	n.i. <sup>b</sup>	16.3 (4.79 ± 0.12)	0.7 (6.14 ± 0.22)
11 <sup>d</sup>		>20	>20	>20	8.9 (5.05 ± 0.14)
12 <sup>e</sup>		14.0 (4.85 ± 0.12)	>20	2.3 (5.63 ± 0.21)	2.4 (5.61 ± 0.18)
13		7.2 (5.14 ± 0.15)	n.i. <sup>b</sup>	n.i. <sup>b</sup>	7.3 (5.13 ± 0.15)
14		>20	>20	>20	9.4 (5.02 ± 0.17)

Table 1 (continued)

ID	Compound	ARTD10/PARP10 IC <sub>50</sub> (μM) (pIC <sub>50</sub> ± SEM <sup>a</sup> )	ARTD8/PARP14 IC <sub>50</sub> (μM) (pIC <sub>50</sub> ± SEM <sup>a</sup> )	ARTD7/PARP15 IC <sub>50</sub> (μM) (pIC <sub>50</sub> ± SEM <sup>a</sup> )	ARTD1/PARP1 IC <sub>50</sub> (μM) (pIC <sub>50</sub> ± SEM <sup>a</sup> )
15		14.0 (4.85 ± 0.13)	>20	>20	5.6 (5.25 ± 0.19)
16		2.9 (5.54 ± 0.15)	>20	1.6 (5.79 ± 0.10)	0.2 (6.71 ± 0.14)
17		2.4 (5.62 ± 0.06)	>20	11.0 (4.96 ± 0.08)	10.5 (4.98 ± 0.08)
18		7.4 (5.13 ± 0.21)	>20	>20	3.7 (5.43 ± 0.15)
19		2.0 (5.70 ± 0.23)	>20	>20	9.7 (5.01 ± 0.11)
20		2.1 (5.68 ± 0.10)	18.7 (4.73 ± 0.19)	>20	0.4 (6.41 ± 0.13)
21		4.6 (5.34 ± 0.15)	>20	16.9 (4.77 ± 0.13)	0.6 (6.23 ± 0.06)
22		>20	>20	>20	0.8 (6.07 ± 0.07)
23		0.8 (6.12 ± 0.11)	1.6 (5.78 ± 0.14)	1.7 (5.76 ± 0.05)	4.4 (5.36 ± 0.16)
24		1.9 (5.72 ± 0.09)	>20	>20	1.1 (5.95 ± 0.06)
25		14.6 (4.84 ± 0.08)	n.i. <sup>b</sup>	n.i. <sup>b</sup>	1.1 (5.97 ± 0.07)
26		6.9 (5.16 ± 0.09)	n.i. <sup>b</sup>	18.0 (4.75 ± 0.07)	0.7 (6.13 ± 0.10)

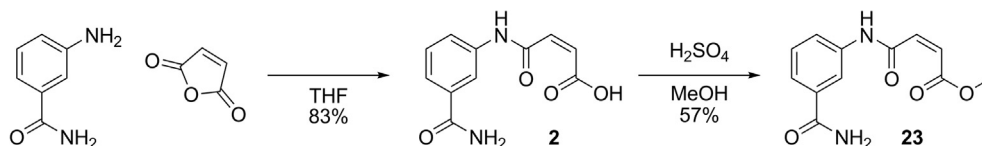
<sup>a</sup> SEM from representative dose-response experiments of two technical replicates.

<sup>b</sup> n.i., no inhibition at 200 μM.

<sup>c</sup> n/a, not applicable compound not soluble under assay conditions.

<sup>d</sup> **11** contained 5% of **12**.

<sup>e</sup> **12** contained 24% of **11**.



**Scheme 1.** Synthetic pathway of a representative mARTD inhibitors.

ease makes it suitable for parallel synthesis of this class of compounds. After evaluation of enzyme inhibition it became clear that the methyl ester and methyl amides all are potent inhibitors of mARTDs (Table 1). The methyl ester (**23**) is the most potent compound but it is indiscriminating with respect to the four enzymes, with  $IC_{50}$  values around 1  $\mu$ M for ARTD7, -8, and -10, and 4.4  $\mu$ M for ARTD1. In addition, the methyl ester is less attractive due to potential ester hydrolysis in cellular systems, a reaction that would produce parent compound **2**. The methyl amides **19** and **20** proved to be bioisosteric and the *cis* configuration in **19** provides selectivity for ARTD10 over ARTD7 and 8, and to some extent over ARTD1. Larger amides in compounds with *cis* configuration (**21** and **22**) reduced potency against ARTD10, -8, and -7 and improved inhibition of ARTD1. The methyl ester **23** and the methyl amides **19** and **20** are as potent as the parent compounds **1** and **2**; the presumed anionic charge of the carboxylic acid is not crucial for inhibition; and the additional hydrogen bond donor present in the amides has limited effect on inhibition. The ketone-containing compounds **24**, **25**, and **26** inhibited ARTD10 and ARTD1 in particular. In general it is clear that small structural modifications can be exploited to affect both potency and selectivity.

The compounds presented here are attractive starting points for a medicinal chemistry program targeting mARTDs due to their lead like properties [23,24]. These generally include a smaller size, lower hydrophobicity, and higher water solubility compared to phase I–III ARTD/PARP inhibitors such as Olaparib (Supplementary Table S10). All presented compounds that display potencies below 10  $\mu$ M have molecular weights below 350, LogP values well below 4, and the numbers of hydrogen bond donors and acceptors are below 4 and 8, respectively. This together with synthetic feasibility and ease of functionalization strongly favors this class of compound for further development into selective mARTD inhibitors.

### 3. Conclusions

We have developed and investigated a set of analogous

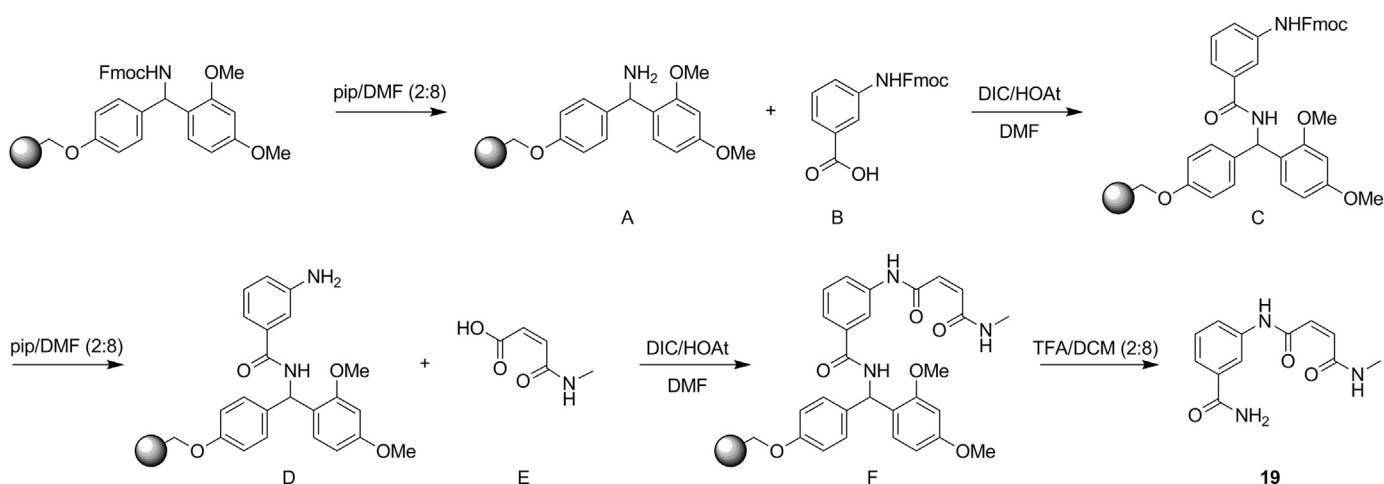
compounds and their inhibition of the catalytic activities of ARTD7, -8 and -10 as well as the dominant clinical target ARTD1. Several new compounds showed an improved potency for one or more ARTDs compared to compounds **1** and **2**. To conclude the SAR analysis, placing the anilide moiety in *para*-position on the benzamide, or alkylating the benzamide, both proved detrimental to enzyme inhibition, suggesting that the interactions between the compounds and the nicotinamide pocket is similar and crucial in both mono- and poly-ARTDs. The carboxylic acid present in the original hit molecules is not crucial for the inhibition. The methyl ester **23** is best suited for targeted inhibition of ARTD7, -8 and -10 while the methyl amide **19** is selective for ARTD10. These are the first reported fully characterized compounds that inhibit the activity of mARTD enzymes and we anticipate that their potencies and selectivity over ARTD1 can be improved. Compound **19** in particular shows promise as a selective ARTD10 inhibitor. The compound class is attractive in terms of both physicochemical properties and synthetic feasibility, which encourages optimization of compound metabolic stability and ARTD isoform selectivity.

### 4. Experimental section

#### 4.1. Chemistry

The majority of compounds included in this study were synthesized starting from aminobenzamides and anhydrides (Scheme 1). These substrates were dissolved in THF and left to stir at room temperature overnight. The precipitates were then collected and dried *in vacuo* to give the desired products. Esterification could then be accomplished by refluxing in methanol with catalytic  $H_2SO_4$ , followed by purification by column chromatography on silica gel. Unless otherwise noted, all compounds had a purity of >95% determined from HPLC. Detailed synthetic procedures and compound characterization are presented in the Supplementary Data.

Compound **19** was synthesized by solid-phase chemistry according to the standard Fmoc protocol [22]. Fmoc deprotection of the RINK-amide resin was achieved through a two-cycles treatment



**Scheme 2.** Solid-phase synthesis of **19**.

with a 20% (v:v) piperidine solution in DMF. Subsequent amide coupling with Fmoc protected 3-aminobenzoic acid (B) was accomplished *via* DIC/HOAt activation. Intermediate C was conveniently converted to F using the same procedures and acid E during the amide coupling step. **19** was then obtained by cleavage of the resin with a 20% (v:v) TFA solution in DCM.

#### 4.2. Recombinant protein production and purification

The cDNA fragments encoding human ARTD1 (full length), ARTD7 (amino acids 459–656, encoding the catalytic domain), ARTD8 (amino acids 1611–1801, encoding the catalytic and WWE domains), and ARTD10 (full length) were inserted into pNIC-Bsa4 [25]. Protein expression in *Escherichia coli* strains BL21(DE3) pRARE, and purification using immobilized metal affinity chromatography followed by size exclusion chromatography (SEC) were carried out as previously described [17] with minor modifications.

#### 4.3. Enzymatic assay

Enzyme automodification was measured essentially as previously described [26]. Briefly, 50- $\mu$ l aliquots of hexahistidine-tagged enzymes (50–200 nM in 50 mM HEPES pH 7.5, 100 mM NaCl, 4 mM MgCl<sub>2</sub>, 0.2 mM TCEP) were immobilized on Ni<sup>2+</sup>-chelating plates (5-PRIME). Compounds were added from stock solutions in DMSO followed by 15 min incubation at 20 °C. The final concentration of DMSO was 1% in all reactions. ADP-ribosyltransferase reactions were started by addition of NAD<sup>+</sup> (2% biotin–NAD<sup>+</sup>; Trevigen) to a concentration below the respective  $K_M$  at 20 °C. After stopping the reactions with 7 M guanidine hydrochloride and washing, assay plates were incubated with streptavidin-conjugated horseradish peroxidase (0.5  $\mu$ g/ml; Jackson Immunoresearch) and chemiluminescence detection was carried out using SuperSignal West Pico (Thermo Fisher Scientific) in a CLARIOstar microplate reader (BMG Labtech). Dose-response experiments were carried out at ten different concentrations in two technical replicate series and 1–4 biological replicates, and were evaluated by three-parameter regression analysis and curve fitting with no further constraints using GraphPad Prism. All reported IC<sub>50</sub> values are best-fit values for representative experiments and are given in  $\mu$ M and the -log IC<sub>50</sub> in molar concentration.

#### Acknowledgments

This work was financed by the Swedish Foundation for Strategic Research (SSF) (RBc08-0014). HS received additional funds from the IngaBritt och Arne Lundbergs Research Foundation, the Swedish Cancer Society, the Swedish Research Council (2012-5247), and the Structural Genomics Consortium.

#### Appendix A. Supplementary data

Supplementary data related to this article can be found at <http://dx.doi.org/10.1016/j.ejmech.2015.03.067>.

#### References

[1] M.O. Hottiger, P.O. Hassa, B. Lüscher, H. Schüler, F. Koch-Nolte, Toward a unified nomenclature for mammalian ADP-ribosyltransferases, *Trends*

*biochem. Sci.* 35 (2010) 208–219.

[2] B.A. Gibson, W.L. Kraus, New insights into the molecular and cellular functions of poly(ADP-ribose) and PARPs, *Nat. Rev. Mol. Cell. Biol.* 13 (2012) 411–424.

[3] E. Barkauskaite, G. Jankevicius, A.G. Ladurner, I. Ahel, G. Timinszky, The recognition and removal of cellular poly(ADP-ribose) signals, *FEBS J.* 280 (2013) 3491–3507.

[4] H. Kleine, E. Poreba, K. Lesniewicz, P.O. Hassa, M.O. Hottiger, D.W. Litchfield, B.H. Shilton, B. Lüscher, Substrate-assisted catalysis by PARP10 limits its activity to mono-ADP-ribosylation, *Mol. Cell.* 32 (2008) 57–69.

[5] S. Vyas, I. Matic, L. Uchima, J. Rood, R. Zaja, R.T. Hay, I. Ahel, P. Chang, Family-wide analysis of poly(ADP-ribose) polymerase activity, *Nat. Commun.* 5 (2014) 4426.

[6] K.L. Feijs, P. Verheugd, B. Lüscher, Expanding functions of intracellular resident mono-ADP-ribosylation in cell physiology, *FEBS J.* 280 (2013) 3519–3529.

[7] M. Kaufmann, K.L. Feijs, B. Lüscher, Function and regulation of the mono-ADP-ribosyltransferase ARTD10, *Curr. Top. Microbiol. Immunol.* 384 (2015) 167–188.

[8] R.C. Aguiar, K. Takeyama, C. He, K. Kreinbrink, M.A. Shipp, B-aggressive lymphoma family proteins have unique domains that modulate transcription and exhibit poly(ADP-ribose) polymerase activity, *J. Biol. Chem.* 280 (2005) 33756–33765.

[9] P. Mehrotra, J.P. Riley, R. Patel, F. Li, L. Voss, S. Goenka, PARP-14 functions as a transcriptional switch for stat6-dependent gene activation, *J. Biol. Chem.* 286 (2011) 1767–1776.

[10] M.B. Iqbal, M. Johns, J. Cao, Y. Liu, S.C. Yu, G.D. Hyde, M.A. Laffan, F.P. Marchese, S.H. Cho, A.R. Clark, F.N. Gavins, K.J. Woollard, P.J. Blackshear, N. Mackman, J.L. Dean, M. Boothby, D.O. Haskard, PARP-14 combines with tristetraprolin in the selective post-transcriptional control of macrophage tissue factor expression, *Blood* 124 (2014) 3646–3655.

[11] P. Verheugd, A.H. Forst, L. Milke, N. Herzog, K.L. Feijs, E. Kremmer, H. Kleine, B. Lüscher, Regulation of NF- $\kappa$ B signalling by the mono-ADP-ribosyltransferase ARTD10, *Nat. Commun.* 4 (2013) 1683.

[12] K.L. Feijs, A.H. Forst, P. Verheugd, B. Lüscher, Macrodomein-containing proteins: regulating new intracellular functions of mono(ADP-ribosylation), *Nat. Rev. Mol. Cell. Biol.* 14 (2013) 443–451.

[13] T. Ekblad, E. Camaioni, H. Schüler, A. Macchiarulo, PARP inhibitors: polypharmacology versus selective inhibition, *FEBS J.* 280 (2013) 3563–3575.

[14] G. Papeo, E. Casale, A. Montagnoli, A. Cirila, PARP inhibitors in cancer therapy: an update, *Expert Opin. Ther. Pat.* 23 (2013) 503–514.

[15] J.L. Riffeil, C.J. Lord, A. Ashworth, Tankyrase-targeted therapeutics: expanding opportunities in the PARP family, *Nat. Rev. Drug Disc.* 11 (2012) 923–936.

[16] N.J. Curtin, C. Szabo, Therapeutic applications of PARP inhibitors: anticancer therapy and beyond, *Mol. Asp. Med.* 34 (2013) 1217–1256.

[17] E. Wahlberg, T. Karlberg, E. Kouznetsova, N. Markova, A. Macchiarulo, A.G. Thorsell, E. Pol, A. Frostell, T. Ekblad, D. Oncu, B. Kull, G.M. Robertson, R. Pellicciari, H. Schüler, J. Weigelt, Family-wide chemical profiling and structural analysis of PARP and tankyrase inhibitors, *Nat. Biotechnol.* 30 (2012) 283–288.

[18] J.D. Steffen, J.R. Brody, R.S. Armen, J.M. Pascal, Structural implications for selective targeting of PARPs, *Front. Oncol.* 3 (2013) 301.

[19] H. Venkannagari, A. Fallarero, K.L. Feijs, B. Lüscher, L. Lehtiö, Activity-based assay for human mono-ADP-ribosyltransferases ARTD7/PARP15 and ARTD10/PARP10 aimed at screening and profiling inhibitors, *Eur. J. Pharm. Sci.* 49 (2013) 148–156.

[20] C.D. Andersson, T. Karlberg, T. Ekblad, A.E.G. Lindgren, A.G. Thorsell, S. Spjut, U. Uciechowska, M.S. Niemiec, P. Wittung-Stafshede, J. Weigelt, M. Elofsson, H. Schüler, A. Linusson, Discovery of ligands for ADP-ribosyltransferases via docking-based virtual screening, *J. Med. Chem.* 55 (2012) 7706–7718.

[21] D.V. Ferraris, Evolution of poly(ADP-ribose) polymerase-1 (PARP-1) inhibitors. From concept to clinic, *J. Med. Chem.* 53 (2010) 4561–4584.

[22] M. Amblard, J.A. Fehrentz, J. Martinez, G. Subra, Methods and protocols of modern solid phase peptide synthesis, *Mol. Biotechnol.* 33 (2006) 239–254.

[23] T.I. Oprea, T.K. Allu, D.C. Fara, R.F. Rad, L. Ostopovici, C.G. Bologna, Lead-like, drug-like or “pub-like”: how different are they? *J. Comput.-Aided Mol. Des.* 21 (2007) 113–119.

[24] P. Workman, I. Collins, Probing the probes: fitness factors for small molecule tools, *Chem. Biol.* 17 (2010) 561–577.

[25] C. Strain-Damerell, P. Mahajan, O. Gileadi, N.A. Burgess-Brown, Medium-throughput production of recombinant human proteins: ligation-independent cloning, *Methods Mol. Biol.* 1091 (2014) 55–72.

[26] M.F. Langelier, D.D. Ruhl, J.L. Planck, W.L. Kraus, J.M. Pascal, The Zn<sub>3</sub> domain of human poly(ADP-ribose) polymerase-1 (PARP-1) functions in both DNA-dependent poly(ADP-ribose) synthesis activity and chromatin compaction, *J. Biol. Chem.* 285 (2010) 18877–18887.